

# Automation of routine elements for spot-scanning proton patient-specific quality assurance

Danairis Hernandez Morales

*Department of Radiation Oncology, Mayo Clinic, Phoenix, AZ 85054, USA*

Jie Shan

*Biomedical Informatics Department, Arizona State University, Scottsdale, AZ 85259, USA*

Wei Liu, Kurt E. Augustine, Martin Bues, Michael J. Davis, and Mirek Fatyga

*Department of Radiation Oncology, Mayo Clinic, Phoenix, AZ 85054, USA*

Jedediah E. Johnson and Daniel W. Mundy

*Department of Radiation Oncology, Mayo Clinic, Rochester, MN 55905, USA*

Jiajian Shen, James E. Younkin, and Joshua B. Stoker<sup>a)</sup>

*Department of Radiation Oncology, Mayo Clinic, Phoenix, AZ 85054, USA*

(Received 24 June 2018; revised 12 September 2018; accepted for publication 7 October 2018; published 20 November 2018)

**Purpose:** At our institution, all proton patient plans undergo patient-specific quality assurance (PSQA) prior to treatment delivery. For intensity-modulated proton beam therapy, quality assurance is complex and time consuming, and it may involve multiple measurements per field. We reviewed our PSQA workflow and identified the steps that could be automated and developed solutions to improve efficiency.

**Methods:** We used the treatment planning system's (TPS) capability to support C# scripts to develop an Eclipse scripting application programming interface (ESAPI) script and automate the preparation of the verification phantom plan for measurements. A local area network (LAN) connection between our measurement equipment and shared database was established to facilitate equipment control, measurement data transfer, and storage. To improve the analysis of the measurement data, a Python script was developed to automatically perform a 2D–3D  $\gamma$ -index analysis comparing measurements in the plane of a two-dimensional detector array with TPS predictions in a water phantom for each acquired measurement.

**Results:** Device connection via LAN granted immediate access to the plan and measurement information for downstream analysis using an online software suite. Automated scripts applied to verification plans reduced time from preparation steps by at least 50%; time reduction from automating  $\gamma$ -index analysis was even more pronounced, dropping by a factor of 10. On average, we observed an overall time savings of 55% in completion of the PSQA per patient plan.

**Conclusions:** The automation of the routine tasks in the PSQA workflow significantly reduced the time required per patient, reduced user fatigue, and frees up system users from routine and repetitive workflow steps allowing increased focus on evaluating key quality metrics. © 2018 American Association of Physicists in Medicine [<https://doi.org/10.1002/mp.13246>]

Key words: IMPT, patient-specific quality assurance, proton therapy, PSQA

## 1. INTRODUCTION

Intensity-modulated proton therapy (IMPT) delivers a highly conformal dose of ionizing radiation by controlling the placement of spots with steering magnets and by varying the kinetic energy of protons to achieve the desired radiological penetration depth. Several reports have commented on the experiences in other institutions of performing patient-specific quality assurance (PSQA) for spot scanning proton beam therapy, describing the need for multiple measurements per field followed by a  $\gamma$ -index analysis on the two-dimensional (2D) dose distributions.<sup>1,2</sup> Various additions to complement PSQA in IMPT have been proposed, such as the use of a second-check dose engine<sup>3</sup> and the use of machine treatment

log files,<sup>4–6</sup> or some combination of the two complemented by measurement.<sup>7</sup> The workflow proposed in this manuscript is a comprehensive approach that incorporates multiple second-check dose engines, a complete log file analysis, as well as dose plane measurements. The innovative automation steps described below allow many aspects of these automated processes to be performed in parallel, thus providing very comprehensive QA to each plan, while still vastly decreasing the amount of time required. The process consists of four principal steps: (a) verification plan preparation, (b) dose measurements, (c) measurement analysis, and (d) machine log files.

With all of the tasks involved in the PSQA process, completing the workflow for each patient is time consuming. Additionally, repetitively performing multistep, complex

tasks required by the aforementioned PSQA workflow may lead to interuser variability and/or process errors. The PSQA workflow was scrutinized for potential improvements in time efficiency and consistency.

### 1.A. Verification plan preparation considerations

Prior to making measurements, patient dose is calculated on a verification image set representing a phantom that holds a 2D ion-chamber array. Then, low-gradient regions within the dose volume of each field are identified for subsequent dose comparisons at various depths.

Although many modern treatment planning systems provide a built-in function to calculate the patient dose on a verification image set, the following step of finding low-gradient regions is typically performed manually. For IMPT PSQA where multiple depths may be measured for each field, defining appropriate measurement locations is tedious and can be very time consuming for complex modulations and/or large fields.

This manuscript details how the Eclipse Scripting Application Programming Interface (ESAPI) may be employed for automated, multi-depth gradient searches to define appropriate sampling points as well as to export the corresponding information to a worksheet for convenience in working at the proton gantries during dose measurements.

### 1.B. Dose measurements

PSQA measurements allow dose comparisons to be performed between each delivered and planned verification field to ensure accurate treatment delivery. For this, 2D ion-chamber arrays have been used to capture the fluence at the depth of interest.<sup>8,9</sup> At our clinic, we employ the MatriXX PT (IBA Dosimetry, Schwarzenbruck, Germany). For each treatment field, the MatriXX PT captures the fluence at multiple depths within an acrylic stack and provides point dose measurements at a location of interest for comparison with our second-check dose engines.

This manuscript describes a procedure developed to perform these measurements more efficiently as well as write the measurement data to a network share drive to enable immediate access to acquired data for analysis.

### 1.C. Measurement analysis

Measured dose planes are analyzed to quantify deviations from the planned dose. At our clinic, manual  $\gamma$ -index analyses, based on Low *et al.*,<sup>10</sup> are performed using Omnipro- $\Gamma$ mRT v1.7 (IBA Dosimetry, Schwarzenbruck, Germany) software. Before the analysis, several manual manipulations (i.e., image orientation, scaling, translation, and delineation of analysis region) were required to rigidly register the measurement and verification plane sets for analysis.

We found that these required manipulations typically extend the task upward of 30 min per plan. However, for

plans with one or more fields larger than the 2D measurement array, these manipulations required as much as 90 min per plan.

On review, we determined these manipulations were identical for each field. This repetitive, multistep sequence of actions promotes user fatigue and creates an opportunity for error and/or interuser variability. We hypothesized that automating these repetitive steps would not only decrease the time required but also reduce interuser variability. This manuscript details the development of an online, automated analysis tool that autoregisters dose planes, including required image reorientation, and subsequently performs the  $\gamma$ -index analyses.

### 1.D. Machine log files

The last component of the PSQA workflow considers the machine log files generated during the measurement step of PSQA. These log files are written locally to the accelerator mainframe interface and accessed after measurements. These files are transferred via USB key to individual workstations for evaluation, which primarily consists of verifying the position and MU of each delivered spot. Access to these files and the analysis script proved cumbersome when multiple users were involved. This manuscript details the development of a secure, automated file transfer protocol as well as the migration of analysis tools to an online portal for a more efficient workflow.

## 2. MATERIALS AND METHODS

### 2.A. Verification plan preparation

The Eclipse interface was used to generate a separate verification plan on a water-equivalent phantom image set for each field, with dose calculated using the treatment planning system dose algorithm. This verification plan was then exported to an in-house web-based script where additional verification dose distributions were calculated using semi-analytical and Monte Carlo algorithms; these additional dose calculations were imported back into Eclipse to facilitate comparison with measured dose planes.

A series of parameters was defined to generate profiles in low-dose gradient regions and select the measurement points with dose at or near prescription level, based on the treatment planning system verification plan. Using these parameters, an ESAPI binary plug-in written in C# was developed to automate the gradient evaluation, dose profile generation, and export during verification plan preparation (see Fig. 1). The possible profile location solutions were constrained to grid positions near the center of the target corresponding to ion-chamber positions in the 2D measurement array.

The measurement depths and an array of profile coordinates were then propagated automatically to the semi-analytical and Monte Carlo<sup>11</sup> verification plan dose calculations. A 2D representation of these profiles was plotted using the

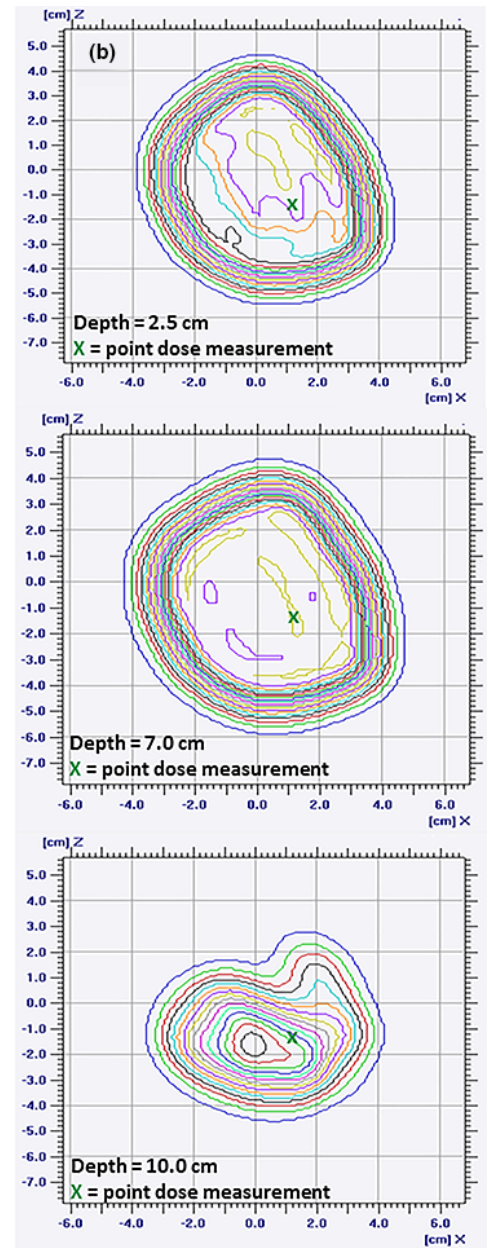
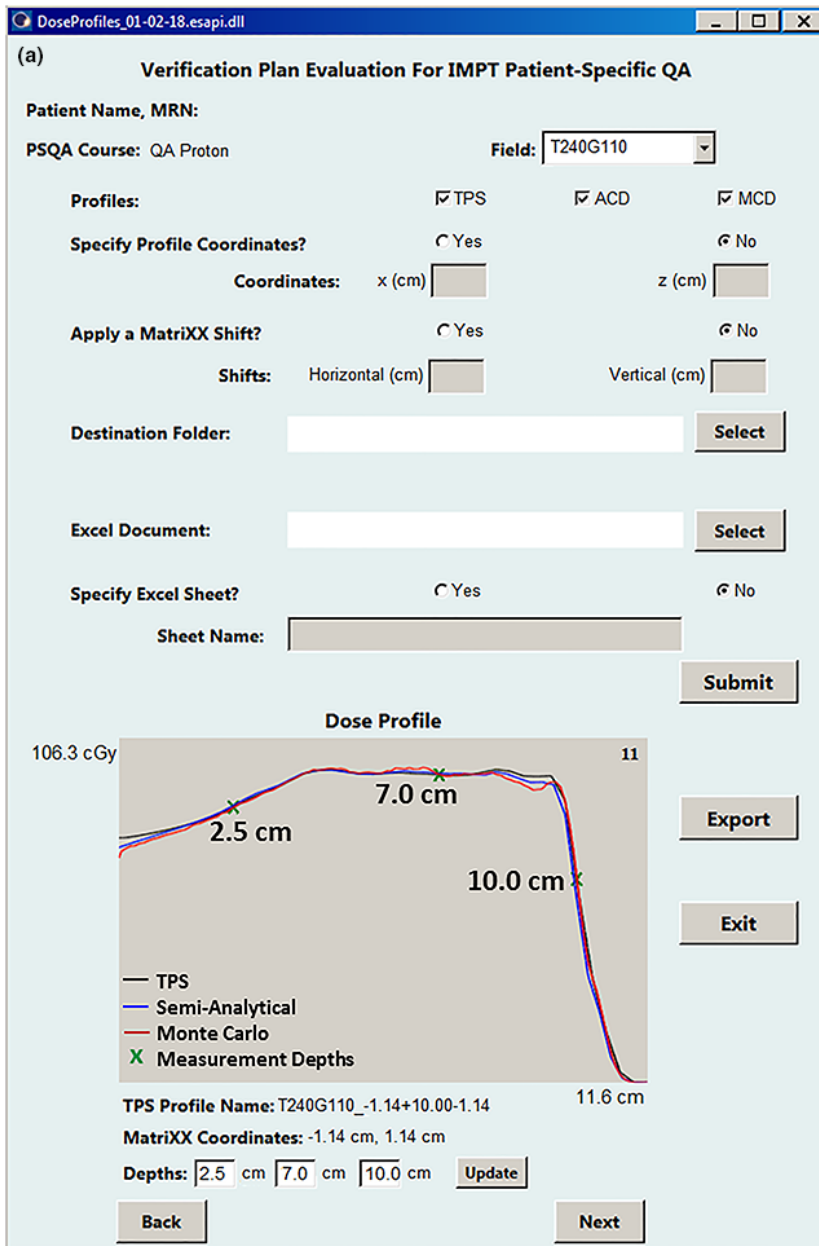


FIG. 1. (a) A gradient evaluation is performed utilizing the ESAPI script on a phantom verification field. With the GUI, the user is able to specify dose profile coordinates or obtain suggested coordinates based on a gradient evaluation algorithm. Additional functions allow the input of lateral detector shifts and directory selection for data export. For Field T240G110 shown here, the depth–dose TPS profile at  $x = -1.14$  cm and  $z = -1.14$  cm from phantom isocenter is suggested for measurements at depths of 2.5, 7.0, and 10.0 cm. This profile location is propagated to the second-check semi-analytical and Monte Carlo profiles for a dose comparison. (b) Point doses, extracted from the 2D array measurement, and dose at each of the selected depths along the beam path are captured for comparison against the planned dose.

ESAPI graphical user interface for user review prior to export to worksheet, as shown in Fig. 1.

## 2.B. Dose measurements

The DigiPhant PT<sup>12</sup> (IBA Dosimetry, Schwarzenbruck, Germany), an acrylic housing designed to hold the MatriXX PT, was employed for its ability to remotely set the measurement depth. The internet protocol addresses (IP) of the DigiPhant’s common control unit (CCU) and MatriXX PT were

changed to facilitate a connection through the clinic’s local area network (LAN). To establish the connection itself, short cable connections from the DigiPhant PT and MatriXX PT to Ethernet ports in the couch replaced those to the manufacturer-provided Ethernet switch. Similarly, a connection to the controlling laptop was established with a short cable connection in the control room with access to the same network location. To securely house all PSQA measurements, the network location was included within the institutional firewall and included a regular backup and maintenance schedule.

The DigiPhant includes etchings in the acrylic housing that facilitated alignment with in-room lasers. The external etchings are located such that when the MatriXX PT was mechanically positioned at a 10-cm water-equivalent depth, the acrylic etchings also align with the MatriXX PT measurement plane etching. The laser alignment allows for setup accuracy of the QA assembly within  $\pm 1$  mm.

### 2.C. Measurement analysis

An in-house Python script was developed to perform an automated 2D–3D<sup>13</sup>  $\gamma$ -index analysis between the individually measured dose planes and the TPS dose volume in water generated by the verification plan. The script included parameters that automated the routine manipulations of the measurement data to prepare it for  $\gamma$ -index analysis: position correction, dose rescaling, image orientation, image resampling, ROI selection, signal threshold, and search step size. The script GUI was accessed through a web application and required the input of the measurement data files, the corresponding DICOM file of verification field dose volume, the daily calibration value of the 2D detector array, a dose tolerance, and the distance to agreement (DTA).

A PDF report summarizing the results of each measurement data file set submitted was automatically generated that included plots of the measurement plane and corresponding verification plane, the total lateral shifts applied to the measurement plane during the image registration, lateral dose profiles at an automatically selected or user-specified position, and the  $\gamma$ -index analyses results. An example report is provided in Fig. 2. The generated reports were used as a component of the final patient quality assurance document.

### 2.D. Machine log files

A script was implemented to perform a secure, automated transfer of the newly available field log files locally stored behind the treatment machine firewall to a network share. The transferred files were uploaded to the web interface which used an in-house developed script to evaluate the MU and lateral positions of each delivered spot against the treatment plan exported earlier during the verification plan preparation stage. A report summarizing the deviations was automatically generated for each treatment field (a sample analysis can be seen in Appendix A) for inclusion in the patient quality assurance document.

### 2.E. Measuring time savings of automated methods

The time spent in the manual PSQA workflow was prospectively measured for 30 treatment plans with 76 fields (approx. 2.5 fields per plan) with varying levels of complexity and covering eight principle disease sites: prostate, lung, esophagus, craniospinal, breast, neck, brain, and spine. The measurements quantified time spent in preparation, measurement, and analysis steps based on disease site, number of

fields, and modulation level. The time measurements were then retrospectively applied to previous to 890 PSQA fields that had been previously prepared and analyzed manually.

After the deployment of the automated methods, process times for preparation, measurement, and analysis were prospectively measured for 42 fields (from 17 plans). Then, the analysis times for an additional set of 39 fields (16 plans) were retrospectively analyzed to perform parallel  $\gamma$ -index analyses with the manual and automated methods to provide one matched-pairs dataset to look at time reduction in the data analysis step.

## 3. RESULTS

### 3.A. Verification plan preparation

The use of the ESAPI script automated the gradient evaluation portion of the verification plan preparation and decreased the time spent in this task from 10–20 min per field to 1–3 min per field for most plans. For the less frequent, very highly modulated treatment fields that required multiple profiles, an additional 2–5 min (total time 3–8 min) was required. This automation effectively reduced the preparation time by at least 50%.

### 3.B. Dose measurement

Use of the DigiPhant instead of the acrylic stack eliminated pauses between field deliveries to manually change the measurement depth, reducing the overall measurement time per patient. The elimination of long cable connections and Ethernet switch simplified equipment setup; setup time was reduced by 10 min. The LAN connection granted all downstream processes access to the measurement data. This permits immediate intercomparison of the TPS, semi-analytical, Monte Carlo, and the measured doses, either by user or automated tool.

### 3.C. Measurement analysis

The automated  $\gamma$ -index analysis greatly reduced the time needed for data analysis. For example, manual  $\gamma$ -index analysis of a three-field, low modulation plan took approximately 30 min; the automated analysis was done in 3 min. A six-field highly modulated plan required approximately 70 min; the automated script reduced this time to 7 min. One order of magnitude reduction on the analysis time was observed for all plan modulation levels, as shown in Table I. Due to the highly significant time reduction, further statistical analysis was not performed on the matched-pairs data subset.

### 3.D. Log file analysis

Automating the transfer of the machine log files with a password-secured script eliminated virus transfer risks, data loss, and other security risks associated with the use of a

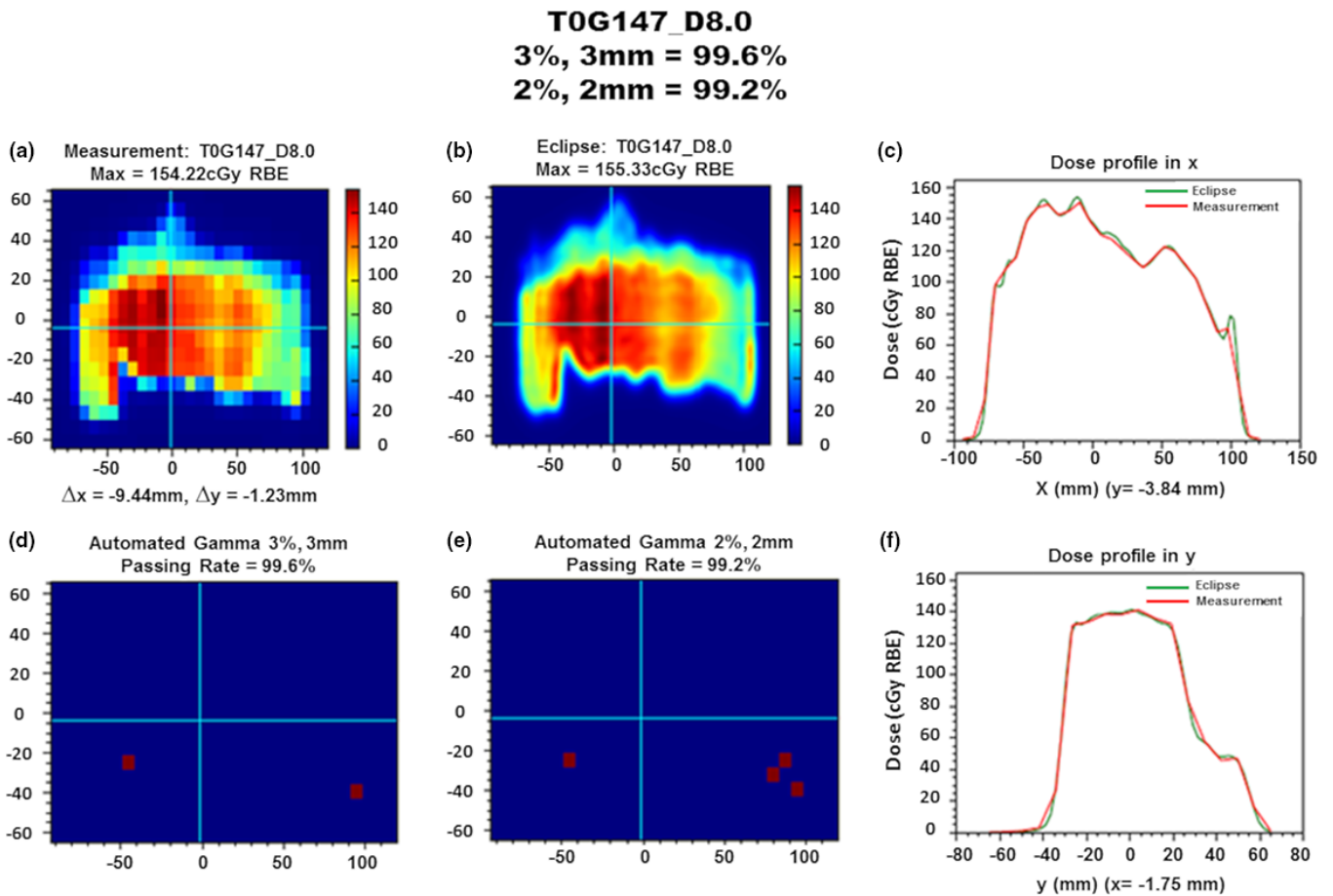


FIG. 2. Automated gamma analysis summary for field T0G147 at a depth of 8.0 cm. (a) Planar dose measurement distribution with total lateral position correction of  $x = -9.44$  mm and  $y = -1.23$  mm. Prior to measurements, the detector was shifted ( $x = 10.0$  mm) to center the dose distribution, so  $x$  shifts by fitting algorithm are determined by delta of reported and detector-shifted values. (b) Planar dose distribution for the verification field at matching prescription depth. (c) Lateral dose profile along the  $x$  direction at  $y = -3.84$  mm. (d) Automated  $\gamma$ -index analysis result with 3%, 3 mm criteria indicating a 99.6% passing rate. (e) Automated  $\gamma$ -index analysis result with 2%, 2 mm criteria indicating a 99.2% passing rate. (f) Lateral dose profile along the  $y$  direction at  $x = -1.75$  mm.

TABLE I. Comparison of required times per field for each task in the manual and automated PSQA procedures. At all modulation levels, automation of the verification plan reduced the time spent by at least 50%. Time needed for PSQA measurements did not directly decrease, but network connectivity allowed the analysis to begin immediately. Automation of the  $\gamma$ -index analysis produced the most significant time reduction of an order of magnitude for all plans.

|                  | Time (min) <sup>a</sup> |           |                     |           |                 |           |
|------------------|-------------------------|-----------|---------------------|-----------|-----------------|-----------|
|                  | Low modulation          |           | Moderate modulation |           | High modulation |           |
|                  | 1–3 fields              |           | 2–4 fields          |           | 4–6 fields      |           |
|                  | Manual                  | Automated | Manual              | Automated | Manual          | Automated |
| Plan preparation | 19 (3)                  | 9 (1)     | 22 (6)              | 8 (1)     | 30 (4)          | 8 (1)     |
| Measurements     | 8 (4)                   | 8 (4)     | 15 (3)              | 15 (3)    | 14 (2)          | 14 (2)    |
| Analysis         | 5 (3)                   | 1 (<1)    | 15 (5)              | 2 (1)     | 19 (3)          | 2 (1)     |
| Overall          | 32 (11)                 | 18 (4)    | 52 (6)              | 24 (4)    | 63 (5)          | 24 (2)    |

<sup>a</sup>Time presented as the average per field with standard deviation in parentheses.

USB drive for everyday file transfers. The script now enables machine log files to be accessed immediately after measurements are completed without the need to perform multiple individual file transfers.

After implementation of the web interface, analysis of machine log files became a routine component of PSQA. Deviations of the spot position and MU of each treatment field were identified in 1–2 min per plan. When deviations

near or past tolerance were identified, the log files facilitated reconstruction of the delivered dose and evaluation of its Dose–Volume Histograms (DVH) against the ones from our commercial TPS. This was used as an additional metric for further evaluation of delivered plan quality.

### 3.E. Overall patient-specific quality assurance time reduction

The time savings from automating the verification plan preparation and  $\gamma$ -index analysis have produced an observable overall time savings in the completion of PSQA for each plan. As observed in Table II, the manual PSQA workflow for a simple plan, such as a prostate treatment plan, was reduced from an average of 32 to 11 min, for an overall time savings of 52%. Similar time savings were observed in more complex plans such as craniospinal treatment plans, which had an overall time savings of 58%. On average, automation decreased the time spent on PSQA tasks by 55%.

## 4. DISCUSSION

Since the deployment of our automated PSQA procedure, we have observed a significant reduction in time required for PSQA. In our clinic, this procedure was implemented in stages due to the diverse skills required, staff involvement, and various time commitments. Because of the simple steps needed and immediate efficiency improvement, the LAN connectivity of the DigiPhant PT and MatriXX PT was established first, followed by the machine log file analysis,  $\gamma$ -index, and ESAPI scripts. In retrospect, it was found that the ESAPI script yielded tremendous time savings with very little development time required. Considering the significant resources and time needed to develop, test, and deploy our  $\gamma$ -index script, we ought to have prioritized efforts on the ESAPI script to have taken advantage of the relatively

immediate time savings while the  $\gamma$ -index script was being developed.

Other centers interested in implementing this approach may readily employ a LAN connection to existing 2D measurement arrays. Verification plan automation may also be employed, depending on the version and manufacture of the facility TPS. Implementing an independent second-check dose engine and web-based tools requires time and expertise that may exist in established facilities with sufficient resources to build a proton center. However, outside academic and/or commercial collaborations may be necessary to create such infrastructure. The authors expect that such investments towards PSQA efficiency are essential for proton centers operating at or near clinical capacity. This manuscript demonstrates that with the proper planning and investment, a thorough PSQA may be carried out for each patient, even under tight time constraints.

The DigiPhant initial setup time was significantly longer than the manual acrylic stack. However, it was found that the additional setup time was compensated for by not having to re-enter the treatment room to adjust measurement depths. For PSQA sessions consisting of four or more fields, measurements were completed in less time with the DigiPhant system.

In spite of the automations, measurements are still the most time-consuming portion of the PSQA workflow. Each institution must evaluate the costs and benefits of this step, for which parallel methods that provide spot-by-spot review, such as log file analysis, are available. At our institution, we have elected to continue 2D array measurements in parallel to log file analysis for two principal reasons: (a) local state regulations require per-patient measurements for all modulated x-ray deliveries, and a similar requirement for IMPT is anticipated, and (b) the 2D array provides a fully independent sampling of beam performance across all beam positions and energies employed for patient treatment.

TABLE II. Comparison of time spent on PSQA procedures per patient plan for various treatment sites with manual and automated workflow components. The number of fields for each site determined from PSQA log of 890 patient fields previously receiving QA. The preparation and analysis time reduction per plan achieved with automation is shown across all disease sites. Measurement time using manual methods was not recorded for this study, so only current measurement times using the DigiPhant assembly are reported here. Consequently, overall PSQA time savings are reported assuming no improvement was made to measurement time.

| Treatment site | Number of fields per plan <sup>a</sup> | Time (min) <sup>a</sup>              |   | Prep/analysis time savings per plan (%) <sup>a</sup> | Time (min) <sup>a</sup> Measurements | Overall time savings (%) <sup>a</sup> |
|----------------|--|--------------------------------------|---|--|--------------------------------------|---------------------------------------|
|                |  | Manual plan preparation and analysis | Automated plan preparation and analysis |  |                                      |                                       |
| Prostate       | 1.1 (0.1)                              | 32 (5)                               | 11 (3)                                  | 65 (6)   | 7 (3)                                | 52 (6)                                |
| Lung           | 2.6 (0.6)                              | 92 (18)                              | 25 (2)                                  | 72 (3)   | 42 (8)                               | 49 (2)                                |
| Esophagus      | 2.4 (0.9)                              | 89 (25)                              | 26 (8)                                  | 71 (1)   | 40 (5)                               | 49 (2)                                |
| Craniospinal   | 3.8 (0.9)                              | 160 (34)                             | 38 (13)                                 | 77 (4)   | 53 (9)                               | 58 (2)                                |
| Breast         | 2.7 (0.8)                              | 106 (12)                             | 26 (5)                                  | 76 (3)   | 36 (10)                              | 57 (5)                                |
| Neck           | 3.0 (1)                                | 148 (43)                             | 33 (8)                                  | 77 (3)   | 53 (7)                               | 56 (5)                                |
| Brain          | 2.4 (0.7)                              | 90 (19)                              | 23 (3)                                  | 75 (3)   | 24 (10)                              | 57 (5)                                |
| Spine          | 2.2 (0.9)                              | 111 (33)                             | 27 (6)                                  | 76 (2)   | 38 (8)                               | 56 (2)                                |

<sup>a</sup>Values presented as the average per plan with standard deviation in parentheses.

The connection to the computer during PSQA measurements could have been established in one of two ways: a closed local network between the MatriXX PT, DigiPhant PT, and a computer, or across our clinic's LAN. We opted for the second option, changing the device's IP addresses to be compatible with our facility's network. This not only eliminated the need to use long cables through the vault maze but also provided immediate access to measured results via the clinic LAN. Because of this approach, analysis could begin immediately after data acquisition and from any location. This also ensured that all PSQA data were stored in a secured, backed up network location from the moment it was acquired. The controller laptop served only to run essential software during data collection. Finally, using the LAN to immediately store PSQA data to a network share laid the groundwork for future automations, such as using a file listener to immediately begin processing measured dose planes and log files.

The ESAPI script enhanced the preparation of all PSQA verification plans by decreasing the time spent performing the gradient evaluation and exporting profile data. However, it was still challenging to use it for the roughly 10% of plans whose treatment volumes required measurement at multiple depths, such as a single field treating both the brain and spine. As the ESAPI script was developed, advanced features were added to help with the preparation of complex plans. These included the ability to browse through alternative depth-dose profiles and export multiple depth-dose profiles. With these features, the user could spend additional time evaluating different regions in the treatment volume to select one or more dose profiles that enable the measurement of all critical depths. In our experience with these complex plans, the additional time required was limited to 2–5 min per field. While the verification plan preparation time savings was reduced for these cases, the ESAPI script still allowed the preparation to be done in less time compared to our manual method. Due to the complex nature of IMPT plans with highly modulated fields, we retained the user-review step for all profile evaluations, which provided flexibility in cases where expert knowledge was required. Future capabilities and improvements to the selection algorithm that will improve depth and dose profile selection for all verification fields will be explored in the future.

The 2D–3D  $\gamma$ -analysis script was developed to facilitate integration into our other IMPT evaluation tools, to generate reports easily, and to simplify code maintenance. Its advanced features gave us the flexibility to specify the manipulation of the dataset before analysis and customize the analysis criteria. An example of these features is the automatic image registration that quickly corrects for both small shifts introduced during the alignment of the DigiPhant and 2D array with the treatment room lasers and the large shifts used in our workflow to capture the lateral extent of fields larger than our 2D array. The inclusion of automatic ROI selection limited the analysis to the measured region and allowed successful analysis of large fields without changes to the workflow.

Our improvements in efficiency relied on the use of a measurement system that allows simple changes in measurement depth and automation of routine procedures in the preparation and analysis stages of the workflow. Additional time efficiency could be achieved through improved equipment designs. For example, a device that could measure dose in three dimensions would enable multiple depth measurements from a single field delivery, decreasing the measurement time per patient by at least 50%. A sealed water tank and detector set would also improve time efficiency by eliminating the need to fill and empty the tank during each PSQA session.

## 5. CONCLUSION

The PSQA workflow at our clinic was analyzed to identify steps that could be improved and automated. Our measurement assembly was designed for remote operation, reducing operator transit time in and out of the treatment room. Use of a LAN connection not only enabled rapid and secure PSQA data storage but also improved access. The ESAPI script streamlined verification plan preparation, and a Python script automated the numerous small and repetitive steps required during  $\gamma$ -index analysis. With the automation of these steps, the time required for PSQA was reduced by more than half. This reduction in the time spent per patient in PSQA has benefited our clinic, especially as patient volume continues to increase.

## ACKNOWLEDGMENTS

The authors wish to thank Dr. Keith Furutani for contributing to the development of the log file script. We also thank Scott P. Shepherd for providing information technology support during the development of the ESAPI script. Finally, we are thankful to Jarrod M. Lentz and Bryce C. Allred for providing feedback on the  $\gamma$ -index analysis and ESAPI scripts. Dr. Wei Liu and Jie Shan were supported by the National Cancer Institute (NCI) Career Development Award K25CA168984, Arizona Biomedical Research Investigator Award, the Lawrence W. and Marilyn W. Matteson Fund for Cancer Research, and the Kemper Marley Foundation.

## CONFLICTS OF INTEREST

The authors have no relevant conflict of interest to disclose.

## APPENDIX A

### LOG FILE ANALYSIS

For each treatment plan, the set of delivered machine log files were exported to our shared network drive and analyzed against the TPS-planned DICOM file after PSQA measurements were completed. For each treatment

field, the MU deviations and position deviations of each delivered spot were compared against their expected values. These deviations were summarized in two plots which included a histogram of the MU differences and the per-spot MU deviation (see Fig. A1). The lateral deviations of each spot from the planned delivery position were also compared and presented in deviation plots identifying the corresponding beam energy layer, energy run average, and tolerances for both lateral beam directions. A more complete description of this log file analysis will be provided in an upcoming publication. In the cases where the spot positions ranged near or outside the tolerances, the machine log files were used to reconstruct a dose volume to evaluate variance in target and organ at risk DVHs.

## APPENDIX B

### 2D–3D GAMMA ANALYSIS

A total of 25 dose planes were obtained from six patient plans with different disease sites and were used to benchmark the 2D–3D  $\gamma$ -index algorithm. Of those 25 planes, three were proximal to, four were distal to, and 18 were at the plateau of the region with the prescription dose. The results were evaluated against our previous manual 2D–2D method by comparing the passing rates of the 3%, 3 mm and 2%, 2 mm  $\gamma$ -index analyses and the distributions of failed pixels.

Consistent with previous reports studying differences between 2D and 3D gamma analyses, results at all depth planes yielded equal or higher passing rates with the

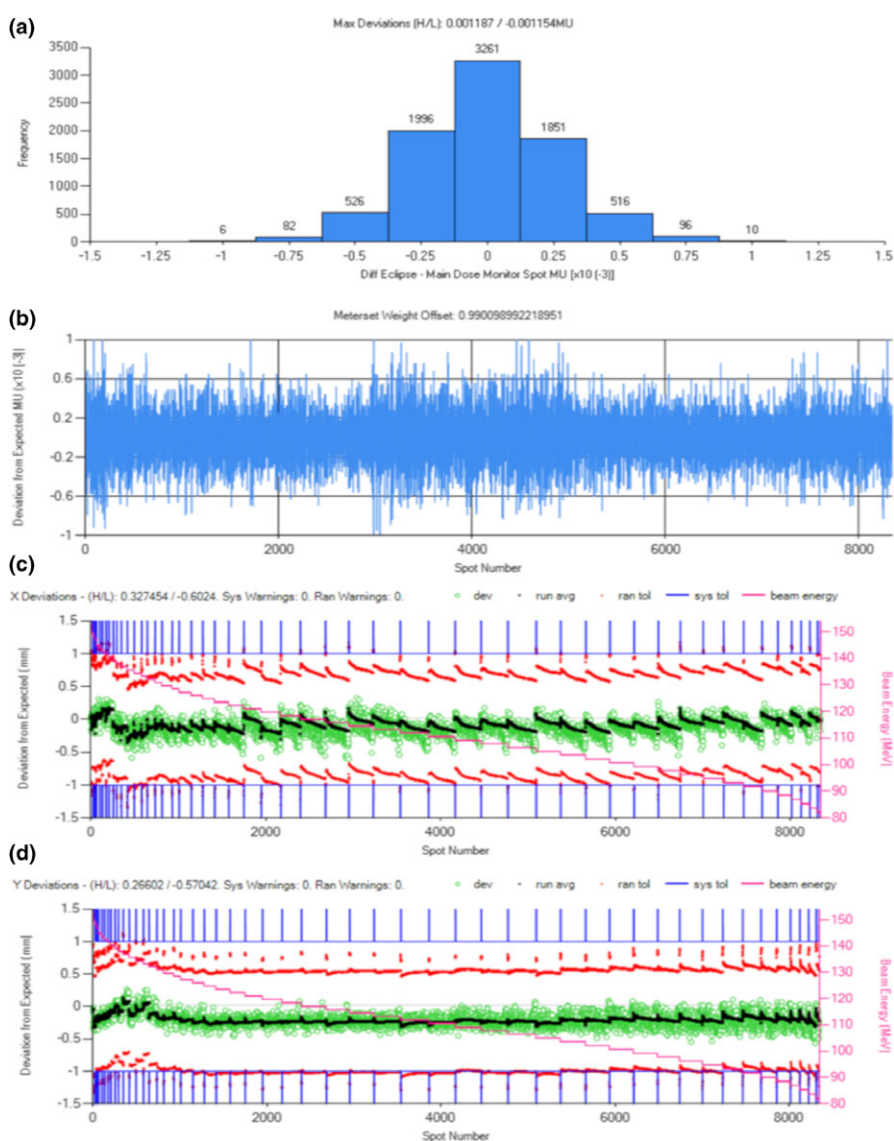


FIG. A1. Log file analysis summary of a treatment field comparing the delivered spot MU and position to the planned version. (a) Histogram of spot MU deviations; (b) per spot MU deviation; (c) the per-spot position (green circles) and average (black dots) deviation in the horizontal aspect of the beams eye view, with systematic error tolerances represented by blue lines, random error tolerances represented by red points, and beam energy indicated by pink stair step and secondary vertical axis values; and (d) similar to (c) except showing the per spot position deviations in the vertical aspect of the beams eye view. [Color figure can be viewed at [wileyonlinelibrary.com](http://wileyonlinelibrary.com)]



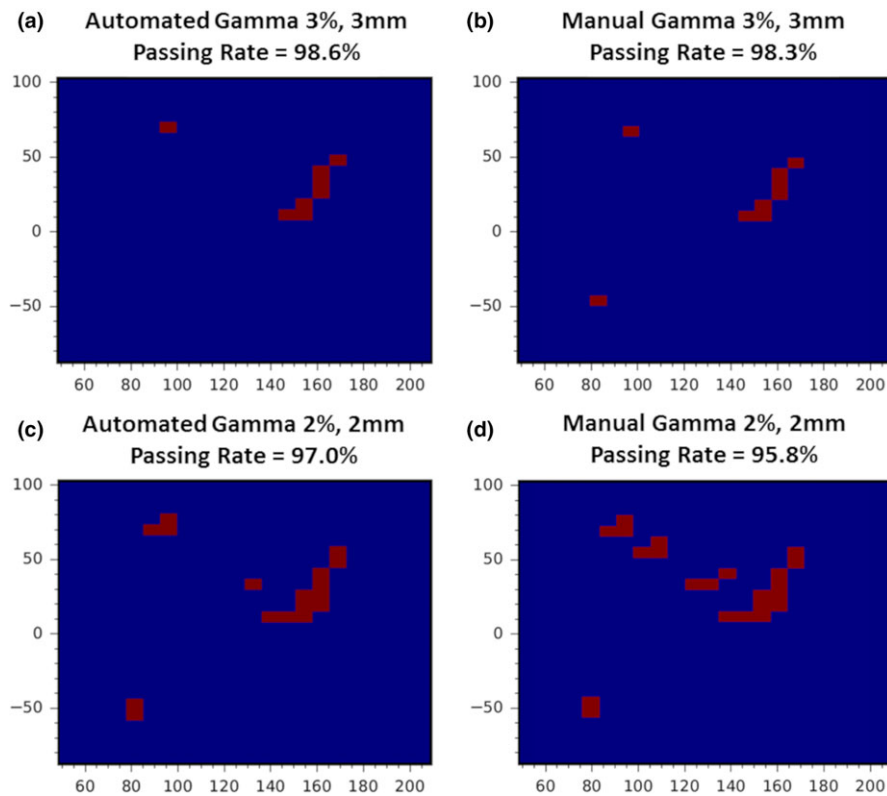


FIG. B1. Automated 2D–3D and manual 2D–2D gamma failed pixel distribution and passing rate comparison for a prescription depth of 4.5 cm. (a) Automated 3%, 3 mm  $\gamma$ -index analysis with passing rate of 98.6%. (b) Manual 3%, 3 mm  $\gamma$ -index analysis with passing rate of 98.3%. (c) Automated 2%, 2 mm  $\gamma$ -index analysis with passing rate of 97.0%. (d) Manual 2%, 2 mm  $\gamma$ -index analysis with passing rate of 95.8%. [Color figure can be viewed at [wileyonlinelibrary.com](http://wileyonlinelibrary.com)]

TABLE BI. Comparison of the automated 2D–3D 3%, 3 mm and 2%, 2 mm  $\gamma$ -index results against the manual 2D–2D 3%, 3 mm and 2%, 2 mm  $\gamma$ -index analysis for a subset of six patient plans at prescription depth. The parallel analysis was performed with identical ROIs and scaling factors based on our detector daily warm-up values.

| Patient | Automated gamma 3%, 3 mm (%) | Manual gamma 3%, 3 mm (%) | Automated gamma 2%, 2 mm (%) | Manual gamma 2%, 2 mm (%) |
|---------|------------------------------|---------------------------|------------------------------|---------------------------|
| 1       | 99.5                         | 98.9                      | 98.3                         | 95.9                      |
| 2       | 100                          | 99.6                      | 100                          | 98.7                      |
| 3       | 100                          | 100                       | 100                          | 100                       |
| 4       | 100                          | 100                       | 99.0                         | 98.8                      |
| 5       | 100                          | 99.9                      | 99.7                         | 99.3                      |
| 6       | 98.6                         | 98.3                      | 97.0                         | 95.8                      |

automated 2D–3D  $\gamma$ -index analysis when compared to the 2D–2D method.<sup>14,15</sup> The difference of the resulting distributions of failed pixels was consistent with the reported passing rates of both methods (see Fig. B1), which verified the differences due to the additional degree of freedom in the 2D–3D  $\gamma$ -index analysis. The results for five prescription depth measurements are included in Table BI

<sup>a)</sup> Author to whom correspondence should be addressed. Electronic mail: [stoker.joshua@mayo.edu](mailto:stoker.joshua@mayo.edu); Telephone: 480-342-0186

## REFERENCES

- Zhu XR, Poenisch F, Song X, et al. Patient-specific quality assurance for prostate cancer patients receiving spot scanning proton therapy using single-field uniform dose. *Int J Radiat Oncol Biol Phys.* 2011;81:552–559.
- Mackin D, Zhu XR, Poenisch F, et al. Spot-scanning proton therapy patient-specific quality assurance: results from 309 treatment plans. *Int J Part Ther.* 2014;1:711–720.
- Mackin D, Li Y, Taylor MB, et al. Improving spot-scanning proton therapy patient specific quality assurance with HPlusQA, a second-check dose calculation engine. *Med Phys.* 2013;40:121708.
- Belosi MF, van der Meer R, Garcia de Acilu Laa P, Bolsi A, Weber DC, Lomax AJ. Treatment log files as a tool to identify treatment plan sensitivity to inaccuracies in scanned proton beam delivery. *Radiother Oncol.* 2017;125:514–519.
- Li H, Sahoo N, Poenisch F, et al. Use of treatment log files in spot scanning proton therapy as part of patient-specific quality assurance. *Med Phys.* 2013;40:021703.
- Scandurra D, Albertini F, van der Meer R, et al. Assessing the quality of proton PBS treatment delivery using machine log files: comprehensive analysis of clinical treatments delivered at PSI Gantry 2. *Phys Med Biol.* 2016;61:1171–1181.

7. Zhu XR, Li Y, Mackin D, et al. Towards effective and efficient patient-specific quality assurance for spot scanning proton therapy. *Cancers*. 2015;7:631–647.
8. Arjomandy B, Sahoo N, Ciangaru G, Zhu R, Song X, Gillin M. Verification of patient-specific dose distributions in proton therapy using a commercial two-dimensional ion chamber array. *Med Phys*. 2010;37:5831–5837.
9. Varasteh Anvar M, Attili A, Ciocca M, et al. Quality assurance of carbon ion and proton beams: a feasibility study for using the 2D MatriXX detector. *Phys Med*. 2016;32:831–837.
10. Low DA, Harms WB, Mutic S, Purdy JA. A technique for the quantitative evaluation of dose distributions. *Med Phys*. 1998;25:656–661.
11. Beltran C, Seum Wan Chan Tseung H, Augustine KE, et al. Clinical implementation of a proton dose verification system utilizing a GPU accelerated Monte Carlo engine. *Int J Part Ther*. 2016;3:312–319.
12. Lin L, Kang M, Solberg TD, et al. Use of a novel two-dimensional ionization chamber array for pencil beam scanning proton therapy beam quality assurance. *J Appl Clin Med Phys*. 2015;16:270–276.
13. Wendling M, Zij LJ, McDermott LN, et al. A fast algorithm for gamma evaluation in 3D. *Med Phys*. 2007;34:1647–1654.
14. Chang C, Poole KL, Teran AV, Luckman S, Mah D. Three-dimensional gamma criterion for patient-specific quality assurance of spot scanning proton beams. *J Appl Clin Med Phys*. 2015;16:381–388.
15. Pulliam KB, Huang JY, Howell RM, et al. Comparison of 2D and 3D gamma analyses. *Med Phys*. 2014;41:021710.